Journal of Cellular Biochemistry 82:225–233 (2001)

Transcriptional State and Chromatin Structure of the Murine Entactin and Laminin γ1 Genes

Y. Chen and J.M. Keller*

Department of Biochemistry and Molecular Biology, Finch University of Health Sciences/The Chicago Medical School, North Chicago, IL 60064

Abstract The positions of nucleosomes in the proximal 5′regions of the coordinately regulated murine entactin/nidogen and laminin γ1 genes have been identified in four different transcriptional states — constitutively off, basal, induced, and constitutively induced. In the entactin gene a 450 base pair (bp) region of open chromatin is present between three positioned nucleosomes and the transcriptional start site in the basal, induced, and constitutively induced states. Additionally there is a 200 bp open chromatin region at ∼−2.1 kbp that is only present in the induced and constitutively induced states. In the laminin γ1 gene, a 650 bp region of nucleosome-free chromatin is present between nucleosomes positioned at ∼ −750 and +120 in all transcriptionally active states. These results suggest that basal co-expression of these genes requires sites present in these near upstream regions. The induction to high levels appears to involve additional sites and possibly the production of new and/or the modification of existing trans-acting factors. J. Cell. Biochem. 82: 225–233, 2001.

Key words: basement membrane; coordinate transcription; laminin; entactin/nidogen

The coordinated transcriptional expression of the genes that encode the major basement membrane proteins has been shown to result from the treatment of murine teratocarcinoma-derived F9 cells with retinoic acid (RA) and dibutyryl cyclic (dbc) AMP [Strickland et al., 1980; Cooper et al., 1983]. However, the mechanism responsible for this co-induction has remained obscure since its discovery some 20 years ago. A requirement for a new protein(s) was demonstrated by the involvement of a cycloheximide-blockable step after treatment [Wang and Gudas, 1988]. Certainly a confounding factor in understanding the underlying mechanism for this co-regulation is the fact that the expression of these genes is governed by multiple mechanisms, as different levels of individual proteins have been observed in different cell types in culture [Oberbäumer and Speth, 1992], at different stages during development [Dziadek and Timpl, 1985], and in different organs in adult animals [Kleinman et al., 1987].

The importance of chromatin structure in transcriptional regulation is underscored by the numerous transcriptional regulatory proteins that have been found to be associated with chromatin remodeling proteins, viz., ATP-dependent chromatin remodeling proteins and histone acetylases and deacetylases [Kingston and Narlikar, 1999]. This fundamental close relationship between chromatin structure and transcriptional regulation explains the general finding that gene regions that are actively involved in transcriptional regulation are usually more accessible to trans-acting factors, as determined by accessibility to DNA degradative probes [Wolffe, 1995]. These types of observations have been reported for the murine β1 and γ1 genes [Chang et al., 1996; Li and Gudas, 1996]. In this report we present nucleosome positions in and general accessibility to the proximal promoters of the murine entactin/nidogen and laminin γ1 genes under four different physiological states, in order to delineate regions of these genes that are most likely to contain elements involved in their co-regulation.

*Correspondence to: J.M. Keller, Department of Biochemistry and Molecular Biology, Finch University of Health Sciences/The Chicago Medical School, 3333 Green Bay Road, North Chicago, IL 60064.
E-mail: kellerj@finchcms.edu

Received 28 November 2000; Accepted 7 February 2001

METHODS

Cell Culture

The cells used in this study were all of murine origin: teratocarcinoma derived F9 stem cells (ATCC #CRL-1720) [Darrow et al., 1990] and M1536-B3 cells [Chung et al., 1977] and a strain of myeloma cells (NIGMS #GM03570E). All cells were grown as previously described [Brauer and Keller, 1989]. The F9 cells were induced with 0.4 μM RA (from a 3 mg/ml stock in DMSO) and 1 mM dbcAMP [from a 0.1 M frozen stock in PBS (8 g/L NaCl; 0.2 g/L KH_2PO_4; 0.2 g/L KCl; 1.15 g/L Na_2HPO_4)]. The cells were split 1:6 after 48 h and harvested 24 h later.

Obtaining Probes by PCR

Probes used in this study were obtained by genomic PCR using the GeneAmp kit (Perkin-Elmer), following the manufacturer's directions. The primer sets used for the PCR reaction were as follows: probe E1 (+211 to +440) tgatcggagaactgagcttctatg (fwd), tgctactggggtgacagacaag (rev); probe E3 (−797 to −585) tgttattcagctttgcttggaccatc (fwd), acagtttgggaatggaggaattgg (rev); probe L2 (−832 to −626) gatccagtcccttggacacctcg (fwd), aggacttggaccctggcccaac (rev); and probe L3 (+388 to +639) aatgccgccttcaatgtgaccg (fwd), caggtgcagcgtgaggttgatgg (rev).

Indirect End Labeling Analysis

The procedure was performed essentially as described by Wu and Cartwright with slight modifications [Cartwright et al., 1983; Cartwright and Elgin, 1989; Wu, 1989; Thoma, 1996]. Briefly, cultured cells were harvested and the cell pellet resuspended in 7 ml of nuclear buffer (60 mM KCl; 15 mM NaCl; 5 mM $MgCl_2$; 0.1 mM EGTA; 15 mM Tris-HCl, pH 7.4; 0.5 mM DTT; 0.1 mM PMSF; 0.3 M glucose) containing 0.2% NP-40 and lysed in a Dounce homogenizer. The crude nuclear preparation was then centrifuged through a nuclear buffer/1.7 M sucrose cushion at 10,000*g* for 20 min at 4°C. The pellet was suspended in methidiumpropyl EDTA (MPE) nuclear buffer (nuclear buffer without $MgCl_2$) and the concentration of nuclei was adjusted to $\sim 1.12 \times 10^8$ nuclei/ml. H_2O_2 was then added to a final concentration of 1 mM. Freshly made MPE–Fe complex, containing an equimolar mixture of MPE and ferrous ammonium sulfate (from a 5 mM stock), was added to a final concentration of 25 μM, followed by DTT to a final concentration of 1 mM. Aliquots of the reaction mixture were removed at 2, 4, 8, 16, and 32 min and the reaction stopped by the addition of 10 μl of 500 mM bathophenanthroline disulfonate. An equal volume of digestion buffer (20 mM EDTA, 1% SDS) containing 200 μg/ml of proteinase K was added and the samples were incubated at 37°C for 2 h with gentle shaking. The samples were then extracted with phenol/chloroform and the DNA recovered by ethanol precipitation. Samples were further digested with S1 nuclease (0.1 U/μg DNA for 1 h at 37°C), using buffer supplied by the manufacturer (Promega, Madison, WI), in order to convert all single stranded nicks into double stranded cuts. The S1 digested samples were then purified again by ethanol precipitation.

Restriction Enzyme Digestion, Southern Blotting, and Hybridization [Ausubel et al., 1999]

Samples of purified DNA (16 μg) were digested to completion with restriction enzymes according to the manufacturer's instructions. Aliquots were then electrophoresed in a 0.9% agarose gel (SeaKem GTG) in TBE buffer (89 mM Tris-borate; 2 mM EDTA). The gel was stained with 0.5 μg/ml ethidium bromide for 10 min and then soaked in 0.25 N HCl for 30 min, 0.5 N NaOH, 1.5 M NaCl for 30 min, and 0.5 M Tris-HCl, pH 7.4, 1.5 M NaCl for 30 min. DNA was then transferred to a nylon membrane (MagnaGraph, MSI) using a PosiBlot pressure blotter (Stratagene). After crosslinking the DNA to the nylon membrane with UV irradiation, the blot was prehybridized in formamide prehybridization/hybridization (FPH) solution [5X SSC (0.75 M NaCl, 75 mM sodium citrate, pH 7.0), 5X Denhardt's solution (0.5 mg/ml Ficoll 400, 0.5 mg/ml polyvinylpyrrolidone, 0.5 mg/ml BSA), 50% (w/v) formamide, 1% SDS, 100 μg/ml denatured salmon sperm DNA] at 54°C overnight. DNA probes were radiolabeled by PCR with slight modifications of published methods [Schowalter and Sommer, 1989; Mertz and Rashtchian, 1994]. Briefly, reaction mixtures containing 10 mM Tris-HCl, pH 8.3; 50 mM KCl; 0.8 mM $MgCl_2$; 0.25 to 25 μM of a primer pair; 10 pmol each of cold dATP, dTTP, and dGTP; 10 pmol [α-^{32}P]dCTP (60 μCi at 6,000 Ci/mmol); and 2 ng template in a total volume of 20 μl were prepared. Each reaction mixture was subjected to 16 thermal cycles with denaturation at 94°C for 1 min, annealing at 60 to 64°C, depending on the primer set, for 2 min, and

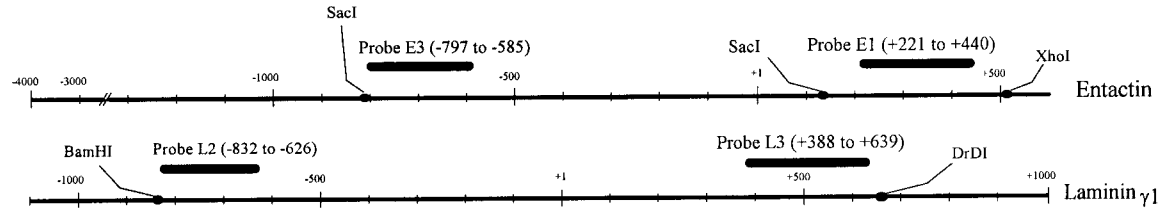

Fig. 1. Positions of DNA probes and selected restriction enzyme sites relative to the transcriptional start sites in the murine entactin and laminin γ1 genes.

extension at 72°C for 6 min. The PCR product was then purified on a G-50 spin column (Boehringer Mannheim) and the radiolabeling efficiency determined by liquid scintillation analysis. After the overnight prehybridization, the solution was changed to fresh FPH containing radiolabeled probe with a specific activity of at least 2×10^9 cpm/μg and incubated at 54°C overnight. The membranes were then washed briefly at room temperature with 0.1X SSC

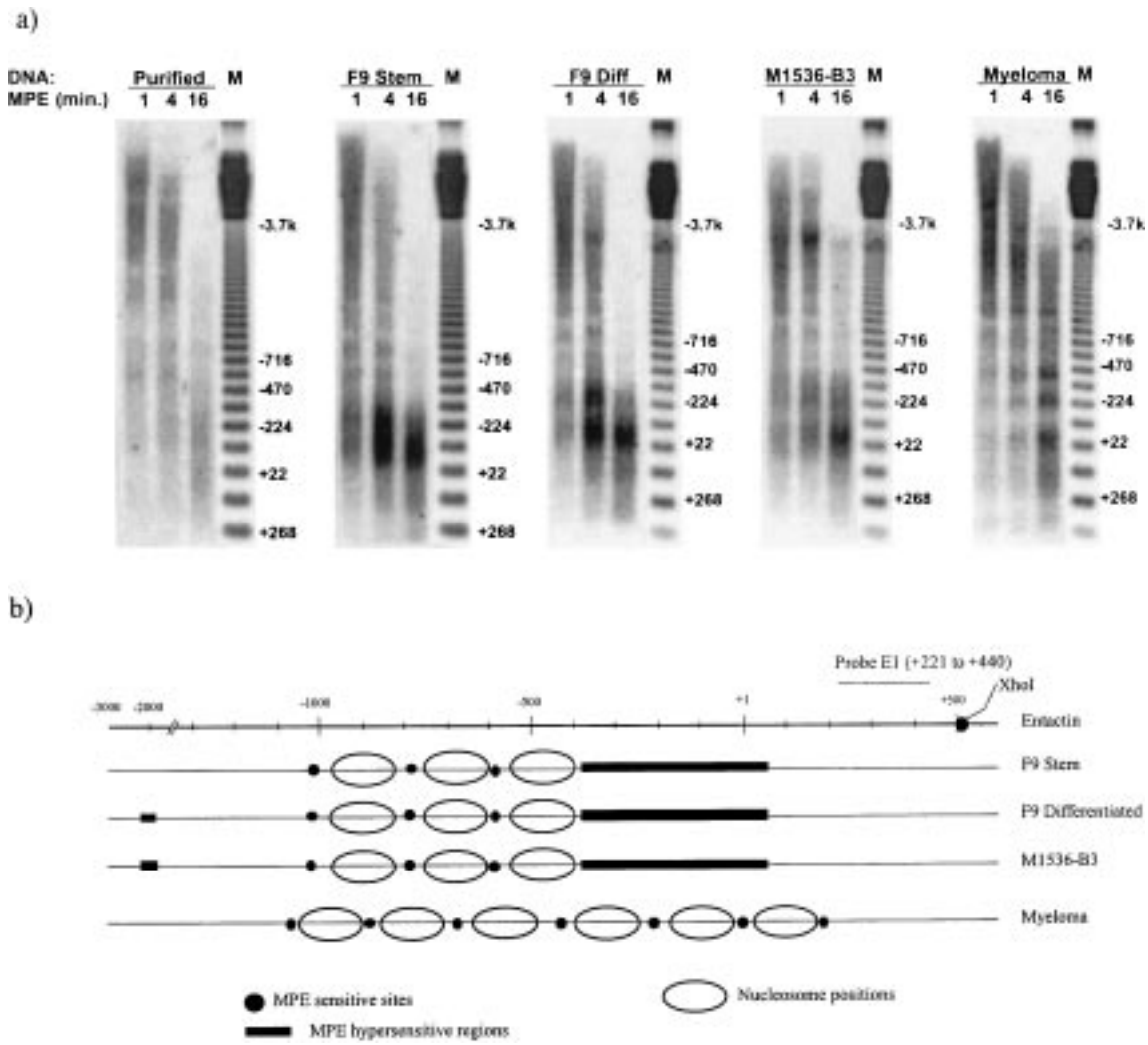

Fig. 2. **a:** Indirect end labeling analysis of the murine entactin gene in F9 stem, F9 differentiated, M1536-B3 and myeloma cells, and DNA purified from M1536-B3 cells, using probe E1 and restriction enzyme XhoI (see Fig. 1). The numbers displayed with the standard gel markers indicate positions relative to the transcription start site of the entactin gene. The analysis of the F9 stem cell was performed on a separate gel, but with a sample of the same digested purified DNA (data not shown). However, the scan of this image is shown in Figure 3. **b:** Schematic diagram of the data. ◀ nucleosome position; ■, upstream hypersensitive region.

containing 0.1% SDS, and then extensively at 68°C in the same buffer. The washed membranes were exposed to X-ray film (Kodak Bio-Max MS) for up to two weeks at −70°C.

Analysis of Indirect End Labeling Data

The developed X-ray films were digitally scanned with a Umax Astra series scanner equipped with a transparency adapter. The digitized images of sample data and molecular weight standards were combined and aligned with Adobe Photoshop 4.0 software. The images were then imported into Molecular Analyst software (Bio-Rad), where the density distributions of the sample data were determined and the standard curves were numerically fitted with a second order polynomial. The data were then imported into Microsoft Excel software, where the final calculations of the sample molecular weights and the plotting of the data were performed. The accuracy of the sample molecular weights determined using this method was estimated to be ∼10%.

RESULTS

Transcriptional Status

Three different murine cell lines were used to provide four transcriptional states with respect to the entactin and laminin γ1 genes. The F9 stem cell represents a basal transcriptional state in which both genes are expressed at a low level. The RA and dbcAMP treated F9 (differentiated F9) cell represents an activated transcriptional state in which both genes are expressed at a high level. The M1536-B3 cell represents a constitutively activated state in which both genes are expressed at a level comparable to that in the induced F9 cell. We initially selected the myeloma cell line to represent the constitutively off state based on its cell type. As judged by the level of mRNA present, it was confirmed that the myeloma cells indeed did not express any detectable amount of entactin transcript (<0.5% of the basal level expressed by the F9 stem cell, data not shown) but did express the laminin γ1 transcript at ∼20% of the F9 stem cell basal level (data not shown). Therefore, the myeloma cell line was used to represent the constitutively repressed transcriptional state for the entactin gene, but a low basal transcriptional state for the laminin γ1 gene.

Chromatin Structure in the 5′ Region of the Murine Entactin Gene

The entactin probe E1 and the restriction enzyme XhoI were used to map the entactin 5′ region upstream from ∼+200 (Fig. 1). As shown in Figures 2a and 3, a similar pattern of chromatin organization from ∼−1,000 to +200 was observed in cells that have a basal level of expression, F9 stem cells, and cells that have a high level of expression, differentiated F9 and M1536-B3. Three MPE sensitive sites, ∼200 bp apart, are present at ∼−1,050, −800, and −600, suggesting the presence of a series of three specifically positioned nucleosomes. In addition, except for a small area of protection at ∼−200 [seen also with micrococcal nuclease (data not shown)], the region between ∼−400 to +50 is MPE hypersensitive. This hypersensitivity to MPE suggests that this region of chromatin has been remodeled in order to allow accessibility by trans-acting factors. The small area of weak protection at ∼−200 is most likely not due to a positioned nucleosome, but rather some other bound protein factor(s). The data also show the presence of a hypersensitive

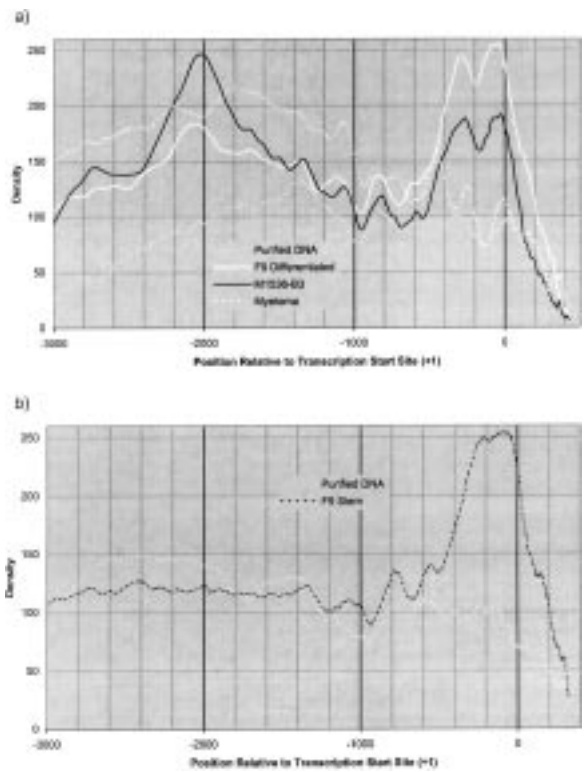

Fig. 3. Digital line scans of the images presented in Figure 2a. Note that although two gels were used, the same digested purified DNA was analyzed on both gels.

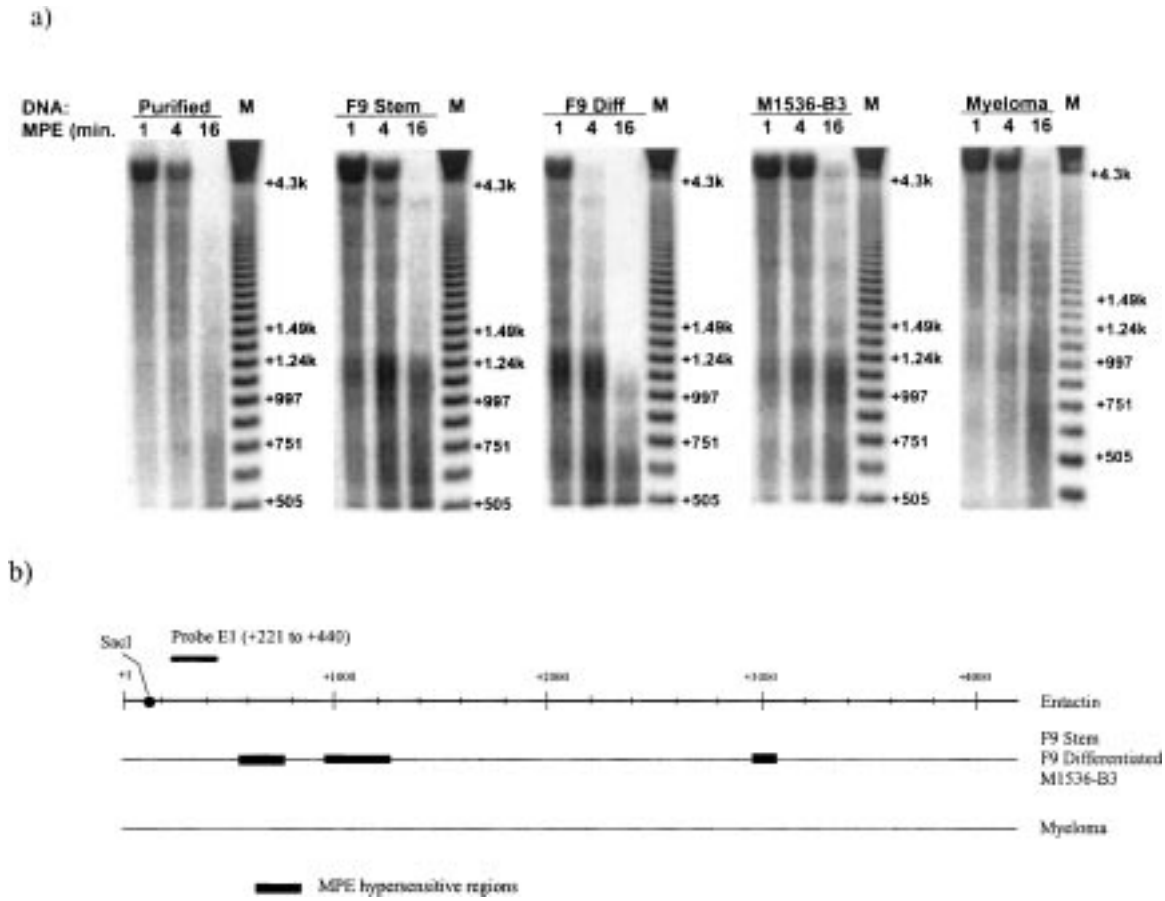

Fig. 4. **a:** Indirect end labeling analysis of the murine entactin gene in F9 stem, F9 differentiated, M1536-B3 and myeloma cells, and DNA purified from M1536-B3 cells, using probe E1 and restriction enzyme SacI (see Fig. 1). The numbers displayed with the standard gel markers indicate positions relative to the transcription start site of the entactin gene. The analyses of the F9 stem and M1536-B3 cells were performed on a separate gel, but with a sample of the same digested purified DNA. However, the scan of this image is shown in Figure 5. **b:** Schematic diagram of the data.

region at ~2.1 kb upstream from the transcription start site in cells that express a high level of entactin, M1536-B3 and differentiated F9, but not in the F9 stem cell, which expresses entactin at a basal level, or the myeloma cell, in which this gene is transcriptionally inactive (Figs. 2a and 3). The same chromatin organization at the entactin core promoter region was found with the use of the upstream probe E3 and the restriction enzyme SacI, which maps the region from ~−600 to +100 (data not shown). A summary schematic of the chromatin structure in the 5′ region upstream of the transcription start site of the murine entactin gene in different transcriptional states is shown in Figure 2b.

The entactin probe E1 and the restriction enzyme SacI (Fig. 1) were used to map the region downstream from ~+600 in the transcribed region (Figs. 4a and 5). Three hypersensitive regions were observed in all three transcriptionally active states. Two of them, at ~+550 to +750 and ~+950 to +1,250, were located close to the transcription start site and the third was further downstream at ~+3 kb. The region from ~+1,250 to +3 kb had very little defined structure that was reproducible. In the myeloma cell, which does not express any detectable level of entactin, the region from ~+600 to +3 kb revealed a lack of well defined chromatin organization. This was in contrast to the same region in cells that express entactin as well as to the promoter region of the myeloma entactin gene. A summary schematic of the chromatin structure in the 5′ region downstream of the transcription start site of the

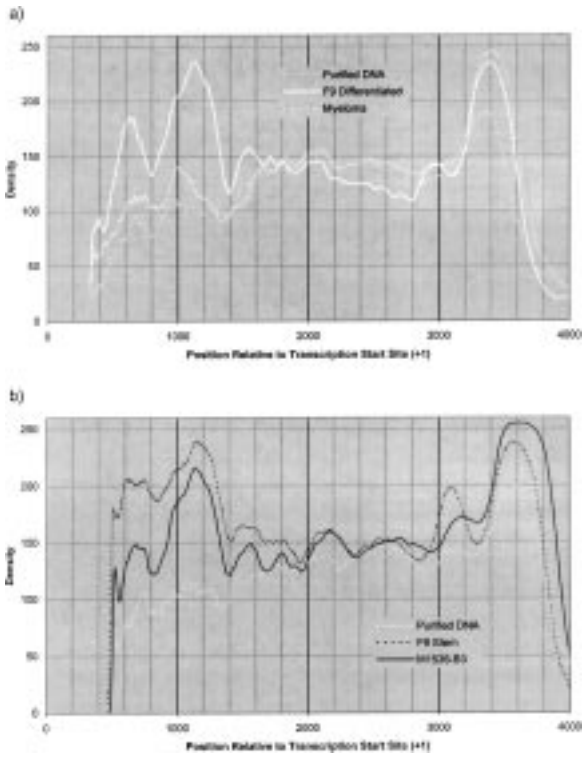

Fig. 5. Digital line scans of the images presented in Figure 4a. Note that although two gels were used, the same digested purified DNA was analyzed on both gels.

murine entactin gene in different transcriptional states is shown in Figure 3b.

Chromatin Structure in the 5′ Region of the Murine Laminin γ1 Gene

The laminin probe L3 and the restriction enzyme DrDI (Fig. 1) were used to map the laminin γ1 gene 5′ region, upstream of the transcription start site (Fig. 6a). The organization of the chromatin in the region between ~−3,000 to +300 was very similar in all transcriptional states studied. A large continuous hypersensitive region was located from ~−600 to +50, which is most intense from ~−400 to +50. This hypersensitive region is flanked on both sides by an area of protection approximately the size of a nucleosome. A summary schematic of the chromatin structure in the 5′ region upstream of the transcription start site of the murine laminin γ1 gene in different transcriptional states is shown in Figure 6b.

The laminin probe L2 and the restriction enzyme BamHI (Fig. 1) were used to map chromatin structure downstream of the transcription start site in the murine laminin γ1 gene (Fig. 7a). The data confirmed the placement of the large hypersensitive region found earlier, from ~−600 to +50 (Fig. 6a), in all of the transcriptional states studied. The small hypersensitive site at ~+200 found previously with the upstream probe (Fig. 6a) is poorly resolved here, appearing as a small shoulder close to ~+100. Additional protected regions are visible further downstream in the transcribed region. These include three hypersensitive sites at ~+400, +600, and +800 in the M1536-B3 cell. These same sites appear to be present in all other transcriptional states studied, although they are much less well defined. There is a strong hypersensitive site at >3.4 kb downstream from the transcription start site in the M1536-B3 cell, but this site is not present in either the F9 stem or F9 differentiated cell. Since this same hypersensitive site was also seen in purified nucleosome-free M1536-B3 DNA (data not shown), but not in that from F9 cells (Fig. 5), it was most likely due to a polymorphic BamH1 restriction site specific to the M1536-B3 cell. Other than the strong hypersensitive site at >3.4 kb in the M1536-B3 cell, there were no clear differences in the chromatin structure from the four transcriptional states. A summary schematic of the chromatin structure in the 5′ region downstream of the transcription start site of the murine laminin γ1 gene in different transcriptional states is shown in Figure 7b.

DISCUSSION

This study was designed to identify specific regions of DNA that could be involved in the known co-regulation of the genes for the major basement membrane proteins. As such, it is an important step along the way to elucidating the overall regulatory mechanism. The results show that the promoter regions of both of these genes have well defined chromatin structure in all transcriptional states studied. The appearance of hypersensitive sites in the 5′ upstream region of the murine entactin gene correlates well with the different transcriptional states studied. In cells that express entactin, either at a basal level, F9 stem, or at a high level, F9 differentiated and M1536-B3, a large accessible region was found at ~−400 to +50, close to the transcription start site, and immediately upstream, between ~−400 to −1050, there were

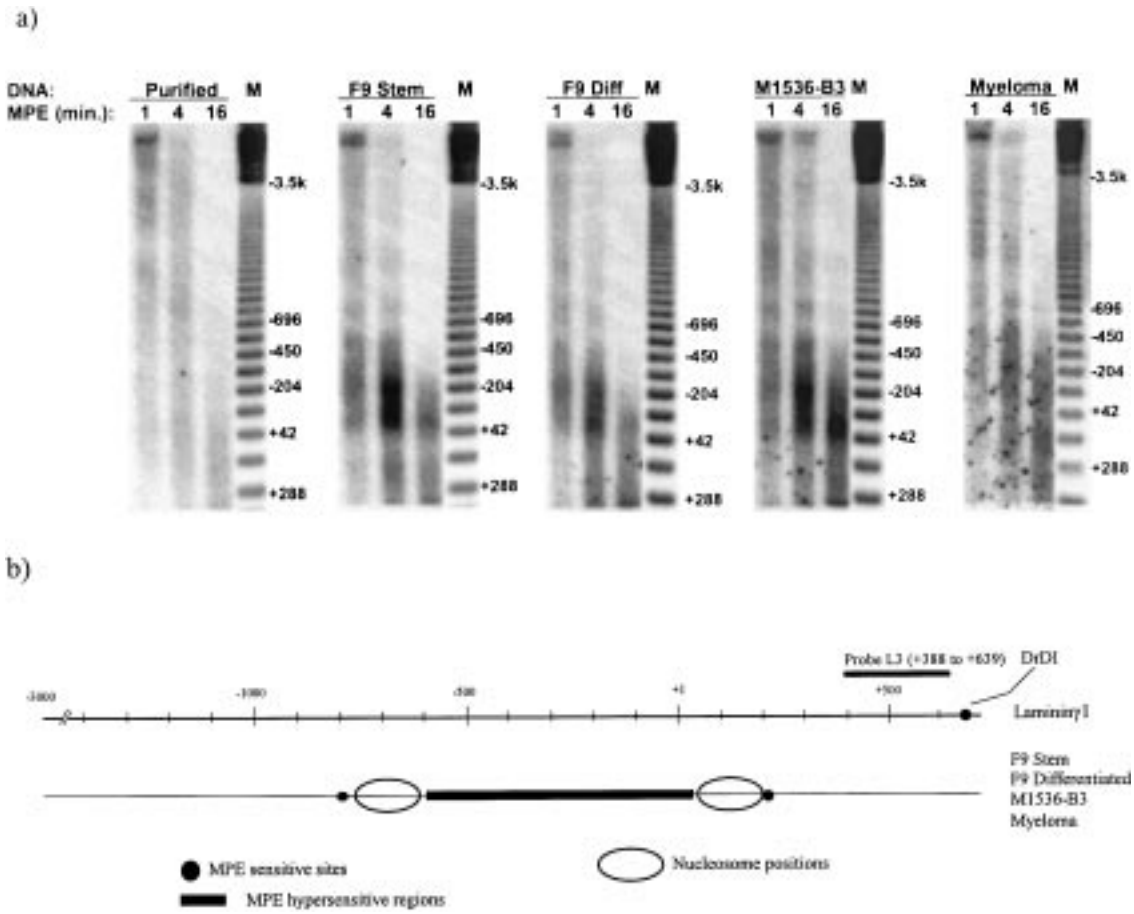

Fig. 6. **a:** Indirect end labeling analysis of the murine laminin γ1 gene in F9 stem, F9 differentiated, M1536-B3 and myeloma cells, and DNA purified from F9 stem cells, using probe L3 and restriction enzyme DrDI (see Fig. 1). The numbers displayed with the standard gel markers indicate positions relative to the transcription start site of the laminin γ1 gene. **b:** Schematic diagram of the data. ◀ nucleosome position.

at least three consecutively positioned nucleosomes. In cells that express entactin at a high level, F9 differentiated and M1536-B3, an additional open chromatin structure was seen further upstream at ∼−2.1 kb. These data suggest that the high expression level of entactin in the F9 and M1536-B3 cells may involve regulatory sequence elements located in the open chromatin regions in the core promoter from ∼−400 to +50 and further upstream at ∼−2.1 kb. However, the core promoter region alone may be adequate for maintaining a basal level of transcription. In contrast, the proximal promoter region (∼−1,000 to +50) of the constitutively off myeloma cell gene is packaged into an array of regularly positioned nucleosomes. This suggests that a specific positioning of nucleosomes may be required to achieve a completely repressed transcriptional state.

Regions of open chromatin structure were also observed downstream of the transcription start site of the entactin gene in cells that expressed entactin either at a basal level, F9 stem, or at a high level, F9 differentiated and M1536-B3. Three hypersensitive regions were observed, at ∼+550 to +750, ∼+950 to +1,250, and at ∼+3 kb, in all of the transcriptionally active states. All three hypersensitive regions were located within the large first intron of the gene, where transcriptional regulatory elements have frequently been found [Burbelo et al., 1988; Haniel et al., 1995]. Thus, these regions of open chromatin could contain additional regulatory sites, e.g., enhancers, involved in the regulation of the entactin gene. In contrast, in the myeloma cell, where the entactin gene is completely repressed, the region downstream of the transcription start

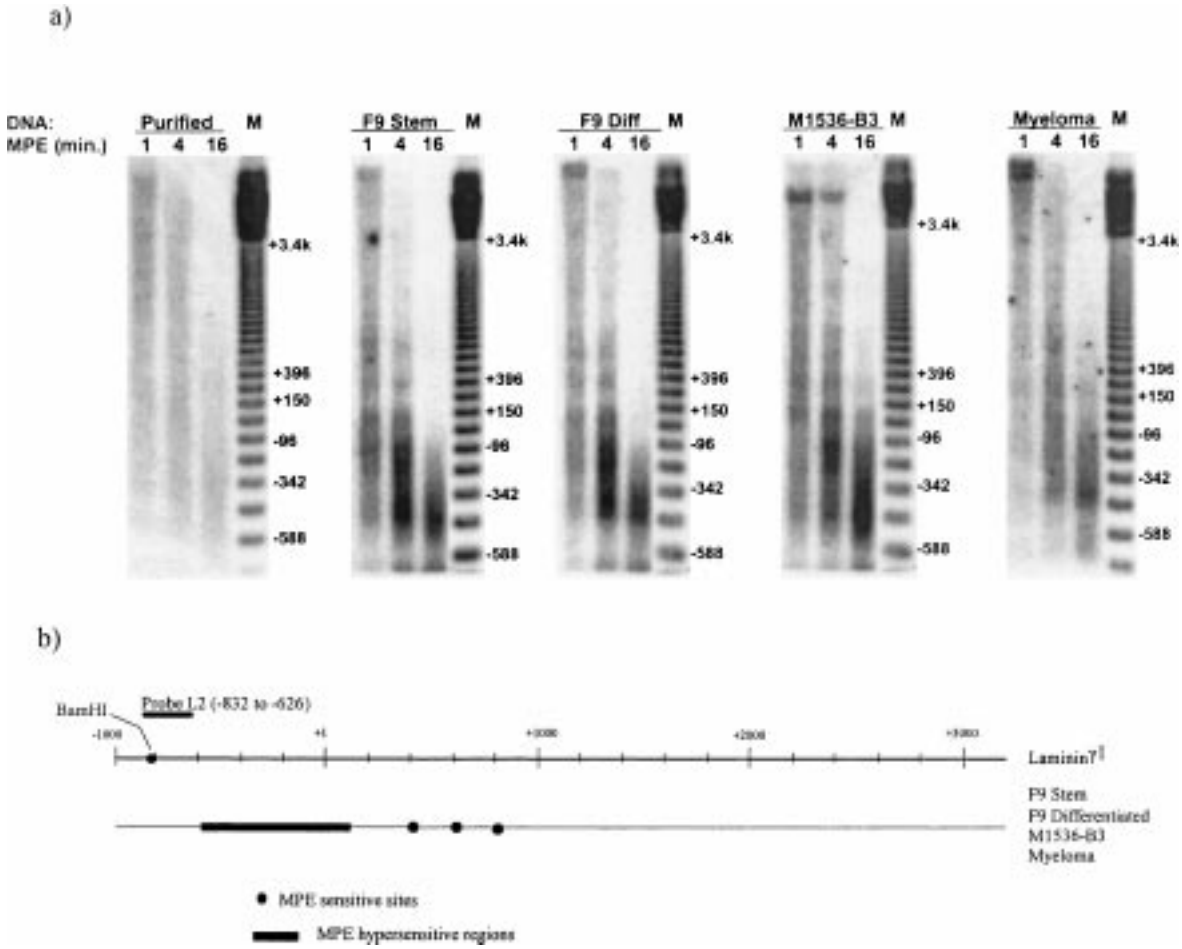

Fig. 7. **a:** Indirect end labeling analysis of the murine laminin γ1 gene in F9 stem, F9 differentiated, M1536-B3 and myeloma cells, and DNA purified from F9 stem cells, using probe L2 and restriction enzyme BamHI (see Fig. 1). The numbers displayed with the standard gel markers indicate the positions relative to the transcription start site of the entactin gene. **b:** Schematic diagram of the data.

site lacked defined chromatin structure. This suggests that the complete suppression of this gene requires only the maintenance of a defined repressive chromatin structure in the promoter region, and not in the transcribed region. A possible mechanism that explains this observation is that a specific repressive chromatin structure, as represented by the array of consecutively positioned nucleosomes, was actively maintained in the upstream region, perhaps by repressor proteins, in order to block any interactions with potential transcription factors. Beyond this region, the specific positioning of nucleosomes are no longer actively maintained and random translational shifts in nucleosome positioning results in the loss of nucleosome alignment within the length of a few nucleosomes.

The 5′ upstream region of the laminin γ1 gene showed identical chromatin organization in all transcriptional states studied. This organization included a large open chromatin region from ∼−600 to +50, flanked on either side by an area of protection approximately the size of a nucleosome. No additional defined structures were found upstream to ∼−3 kb. Downstream from the transcription start site, three additional small hypersensitive sites at ∼+400, +600, and +800, were also present in all of the transcriptional states studied. No additional defined structures were seen further downstream to ∼+3 kb. The large open chromatin region between ∼−600 and +50 in the F9 stem and the F9 differentiated cells has been previously reported [Chang et al., 1996]. In addition, these same investigators reported the

presence of hypersensitive sites at ~+3 kb, +5 kb, and +12.5 kb. The ~+3 kb site was not seen in our own mapping studies, possibly because it is a weak hypersensitive site and lies at the far edge of our detection range, where the sensitivity of the assay is low. All of the hypersensitive sites found in our studies were present in cells that express laminin γ1 at either a basal or a high level. These observations suggest that the chromatin organization observed in these cells is capable of supporting both a basal and a high level of gene expression and that the modulation of expression levels may be determined only by interactions with available transacting factors, which is consistent with a reported change in the fine structure of the hypersensitive site at ~+12.5 kb in response to differentiation of the F9 stem cell [Chang et al., 1996]. However, the possibility that additional regulatory sites are located outside of the studied regions cannot be excluded.

ACKNOWLEDGMENTS

The authors thank Dr. K. Neet for his enthusiastic support of this project.

REFERENCES

Ausubel FM, Brent R, Kingston RE, Moore DD, Seidman JG, Smith JA, Struhl K. 1999. Current protocols in molecular biology. New York: Wiley Interscience.

Brauer PR, Keller JM. 1989. Ultrastructure of a model basement membrane lacking type IV collagen. Anat Rec 223:376–383.

Burbelo PD, Martin GR, Yamada Y. 1988. α 1(IV) and α 2(IV) collagen genes are regulated by a bidirectional promoter and a shared enhancer. Proc Natl Acad Sci USA 85:9679–9682.

Cartwright IL, Elgin SC. 1989. Nonenzymatic cleavage of chromatin. Methods Enzymol 170:359–369.

Cartwright IL, Hertzberg RP, Dervan PB, Elgin SC. 1983. Cleavage of chromatin with methidiumpropyl-EDTA iron(II). Proc Natl Acad Sci USA 80:3213–3217.

Chang HS, Kim NB, Phillips SL. 1996. Positive elements in the laminin γ 1 gene synergize to activate high level transcription during cellular differentiation. Nucleic Acids Res 24:1360–1368.

Chung AE, Estes LE, Shinozuka H, Braginski J, Lorz C, Chung CA. 1977. Morphological and biochemical observations on cells derived from the in vitro differentiation of the embryonal carcinoma cell line PCC4-F. Cancer Res 37:2072–2081.

Cooper AR, Taylor A, Hogan BL. 1983. Changes in the rate of laminin and entactin synthesis in F9 embryonal carcinoma cells treated with retinoic acid and cyclicAMP. Dev Biol 99:510–516.

Darrow AL, Rickles RJ, Strickland S. 1990. Maintenance and use of F9 teratocarcinoma cells. Methods Enzymol 190:110–117.

Dziadek M, Timpl R. 1985. Expression of nidogen and laminin in basement membranes during mouse embryogenesis and in teratocarcinoma cells. Dev Biol 111:372–382.

Haniel A, Welge-Lussen U, Kühn K, Pöschl E. 1995. Identification and characterization of a novel transcriptional silencer in the human collagen type IV gene COL4A2. J Biol Chem 270:11209–11215.

Kingston RE, Narlikar GJ. 1999. ATP-dependent remodeling and acetylation as regulators of chromatin affinity. Genes Dev 13:2339–2352.

Kleinman HK, Ebihara I, Killen PD, Sasaki M, Cannon FB, Yamada Y, Martin GR. 1987. Genes for basement membrane proteins are coordinately expressed in differentiating F9 cells but not in normal adult murine tissues. Dev Biol 122:373–378.

Mertz LM, Rashtchian A. 1994. Nucleotide imbalance and polymerase chain reaction: effects on DNA amplification and synthesis of high specific activity radiolabeled DNA probes. Anal Biochem 221:160–165.

Li C, Gudas LJ. 1996. Murine laminin B1 gene regulation during the retinoic acid- and dibutyryl cyclic AMP-induced differentiation of embryonic F9 teratocarcinoma stem cells. J Biol Chem 271:6810–6818.

Oberbäumer I, Speth C. 1992. Evaluation of mRNA steady-state and protein levels for basement membrane proteins in cultured murine cells. Cell Tissue Res 268:439–445.

Schowalter DB, Sommer SS. 1989. The generation of radiolabeled DNA and RNA probes with polymerase chain reaction. Anal Biochem 177:90–94.

Strickland S, Smith KK, Marotti KR. 1980. Hormonal induction of differentiation in teratocarcinoma stem cells: generation of parietal endoderm by retinoic acid and dibutyryl cAMP. Cell 21:347–355.

Thoma F. 1996. Mapping of nucleosome positions. Methods Enzymol 274:197–214.

Wang SY, Gudas LJ. 1988. Protein synthesis inhibitors prevent the induction of laminin B1, collagen IV (α 1), and other differentiation-specific mRNAs by retinoic acid in F9 teratocarcinoma cells. J Cell Physiol 136:305–311.

Wolffe A. 1995. Chromatin, 2nd Edition. New York: Academic Press. p 199–208.

Wu C. 1989. Analysis of hypersensitive sites in chromatin. Methods Enzymol 170:269–289.